# Highly Potent 4-Amino-indolo[2,3-*c*]azepin-3-one-Containing Somatostatin Mimetics with a Range of sst Receptor Selectivities

Debby Feytens,[†] Magali De Vlaeminck,[†] Renzo Cescato,[‡] Dirk Tourwé,*[,†] and Jean Claude Reubi[‡]

*Department of Organic Chemistry, Vrije Universiteit Brussel, Pleinlaan 2, B-1050 Brussels, Belgium, Division of Cell Biology and Experimental Cancer Research, Institute of Pathology, University of Berne, Berne, Switzerland*

*Received September 23, 2008*

The synthesis, biological evaluation, and conformational analysis of 4-amino-indolo[2,3-*c*]azepin-3-one (Aia)-containing SRIF mimetics are reported. Different subtype selectivities are observed depending on the *N*- and *C*-terminal substituents of the D-Aia-Lys dipeptide mimetic. An $sst_5$-selective analogue with subnanomolar binding affinity was obtained that is the most potent agonist reported to date. A nonselective mimetic with high potency was also identified. This study allows a better definition of the bioactive conformation of the essential D-Trp side chain in the somatostatin pharmacophore.

## Introduction

Somatotropin release-inhibiting factor (SRIF[a]) or somatostatin is an endogenous cyclic tetradecapeptide. It was discovered by Brazeau et al.[1] in 1973 as a potent inhibitor of growth hormone secretion. Somatostatin occurs in two forms, SRIF-14 (14 amino acids) and SRIF-28 (28 amino acids), and is widely distributed throughout the endocrine and central nervous systems and peripheral tissues. SRIF exhibits several physiological functions such as modulation of the release of growth hormone, insulin, glucagon, and gastric acid.[2−4] Moreover, it has been shown to have potent antiproliferative effects and neurotransmitter activities.[5]

The effects of SRIF are mediated by five G-protein coupled receptors, $sst_{1-5}$, which have all been cloned and characterized.[6]

Because of the numerous biological functions of SRIF, selective ligands can be important in the treatment of various human diseases.

SAR studies on a large number of analogues revealed that the Phe[7]-Trp[8]-Lys[9] sequence (numbering of the residues follows that of native SRIF) is critical for biological recognition.[7,8] Several cyclic hexa- and octapeptide analogues containing a D-Trp[8]-Lys[9] sequence have been synthesized[9−11] and developed for clinical use, including octreotide (D-Phe-*c*[Cys-Phe-D-Trp-Lys-Thr-Cys]-Thr-ol). Their poor oral availability and rapid proteolysis are major drawbacks for their clinical use. Therefore, extensive research toward nonpeptide analogues that are selective for each receptor subtype was carried out over the past decade.[12] The critical side chains of the Phe[7]-Trp[8]-Lys[9] sequence were displayed successfully on a variety of nonpeptide scaffolds.[13−15]

A series of analogues, based on the constrained D-Trp-scaffold D-Aia **1**, was developed in our group,[16] and tests on the five SRIF receptors revealed a new, highly potent $sst_{4-5}$ selective SRIF mimetic **2**. The changes in affinity observed for the related analogue **3** suggested that subtype selectivity could be modulated by modifications of the *N*- and *C*-terminal substituents (Figure 1).

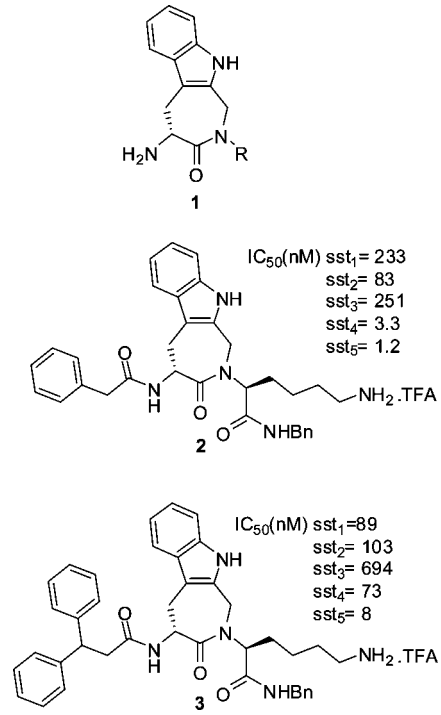


**Figure 1**

To improve the affinity and selectivity, various new analogues were designed by varying the *N*- and *C*-terminal substituents in mimetics **2** and **3**. The phenylacetyl or diphenylpropionyl substituent was varied by removing a phenyl or a methylene group, whereas the *C*-terminal benzyl amide was either elongated or replaced by a (*S*)- or (*R*)-1-phenylethyl amide or a 1-(aminomethyl)naphtalene. Various *N*-substitutions in the D-Trp-Lys or D-$\beta$-Me-Trp-Lys scaffolds developed by Merck have been reported to result in a high $sst_2$ affinity. These include a 4-phenylbenzoyl substituent[17] and urea derivatives of a benzimidazolonepiperidine,[18] 4-spiroindanylpiperidine,[18,19] and *N*-substituted piperazines or isonipecotic acid,[17,20] which mostly target the Phe[7] binding site. We have introduced these variations in

* To whom correspondence should be addressed. Phone: 32-2-629-3295. Fax: 32-2-629-3304. E-mail: datourwe@vub.ac.be.

[†] Vrije Universiteit Brussels.

[‡] University of Berne.

[a] Abbreviations: SRIF, somatostatin; Aia, 4-amino-indolo[2,3-*c*]azepin-3-one; EDC, 1-(3-dimethylaminopropyl)-3-ethylcarbodiimide; NMM, *N*-methylmorpholine; TBTU, *O*-(benzotriazol-1-yl)-*N*,*N*,*N*′,*N*′-tetramethyluronium tetrafluoroborate; EBAW, EtOAc:*n*-BuOH:AcOH:$H_2O$ 1:1:1:1); DMEM, Dulbecco's modified Eagle's medium; GDP, guanidine diphosphate; BSA, bovine serum albumin.

10.1021/jm801205x CCC: $40.75 
Published on Web 12/09/2008

**Scheme 1**[a]

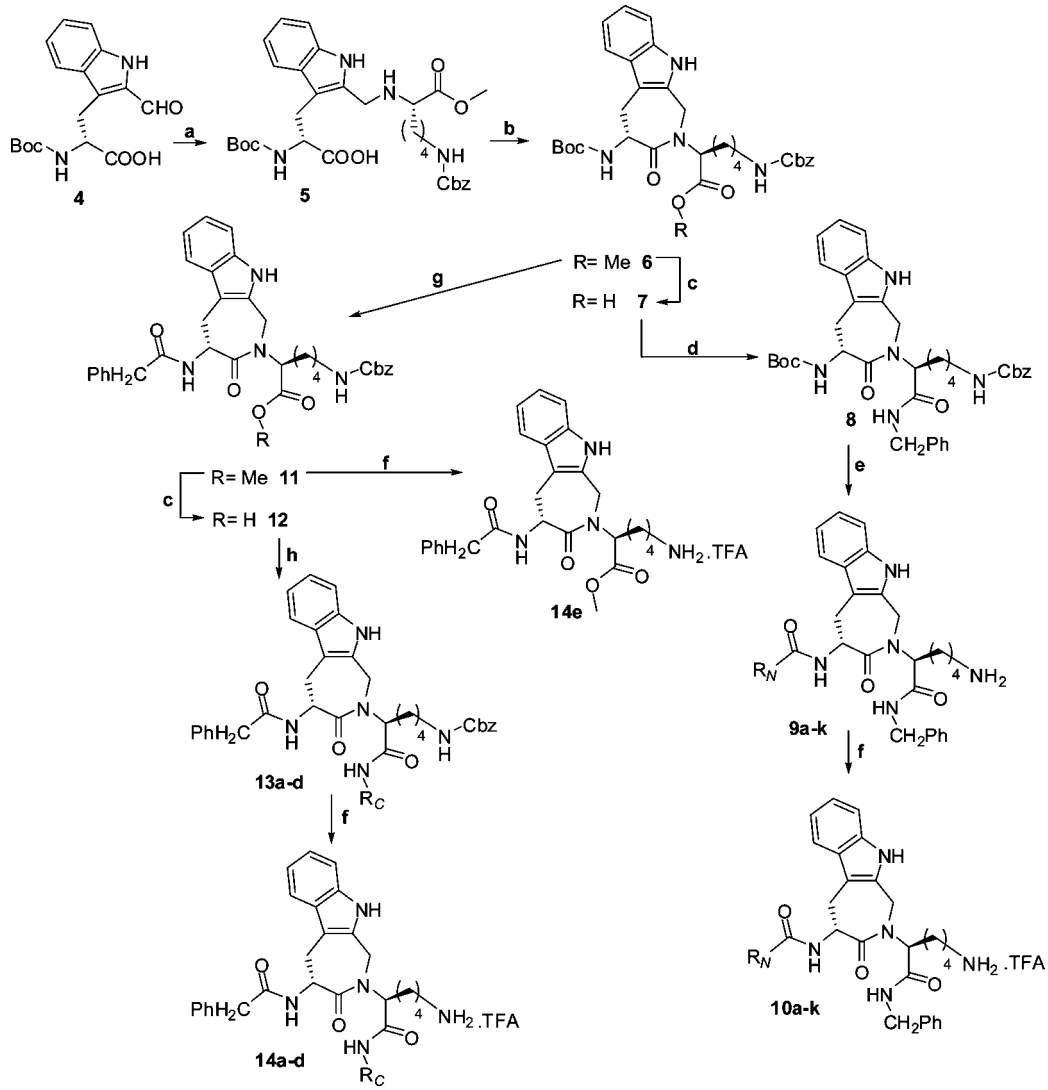


[a] Reagents and conditions: (a) Lys(Cbz)OMe, $CH_2Cl_2$, NMM, pH 6, $MgSO_4$, $NaBH_3CN$, 2 h; (b) EDC, pyridine, $CH_3CN$:$H_2O$ 1:1, high dilution, overnight; (c) MeOH, LiOH, 1.5 h; (d) $PhCH_2NH_2$, $CH_2Cl_2$, $Net_3$, TBTU, pH 8, 1 h; (e) 1.0.5% $H_2O$ in TFA:$CH_3CN$ 2:1, 1 h, 2.*N*,*N*′-disuccinimidyl carbonate, *N*,*N*′diisopropylethylamine, $CH_2Cl_2$, 30 min, followed by $R_NNH_2$ or **2**. $R_NCOOH$, $CH_2CL_2$, $Net_3$, TBTU, pH 8, 1 h; (f) EtOH, HCl, 10% Pd/C, $H_2$, 50 psi or 36% HBr in AcOH, 1 h; (g) (1) 0.5% $H_2O$ in TFA:$CH_3CN$ 2:1, 1 h; (2) $PhCH_2COOH$, $CH_2Cl_2$, $NEt_3$, TBTU, pH 8, 1 h; (h) $CH_2Cl_2$, $Net_3$, TBTU, $R_CNH_2$, pH 8, 1 h.

peptidomimetic **2**. The best analogues in respect of binding affinity and selectivity were functionally tested for agonism and antagonism.

## Results

Two series of analogues were synthesized. In a first set, the *C*-terminal benzyl amide was retained and the *N*-terminal acyl group was changed (Scheme 1, **10a**−**k**), whereas in the second set, the *N*-terminal phenylacetyl group was kept constant while the *C*-terminal part was varied (Scheme 1, **14a**−**e**). Furthermore, the influence of the configuration of the Lys residue in these dipeptide mimetics was investigated (Scheme 2, **18**).

**Synthesis.** Analogues **10a**−**k** and **14a**−**d** were synthesized as shown in Scheme 1. Boc-2′-formyl-D-tryptophan **4** was prepared by $SeO_2$ oxidation of 2-(*tert*-butoxycarbonyl)-2,3,4,9-tetrahydro-1*H*-beta-carboline-3-carboxylic acid (Boc-D-Tcc) as described previously.[21] Reductive amination with ε-Cbz-protected lysine methyl ester and $NaBH_3CN$, immediately followed by cyclization using EDC/pyridine, yielded **6**. In contrast to our previous findings,[16] the cyclization was complete after overnight stirring. For the *C*-terminal variations set of analogues, Boc-protection was removed first, followed by coupling to phenyl acetic acid, yielding **11**. After saponification of the methyl ester in **11**, various amines (Table 1) were coupled, followed by Cbz-removal to **14a**−**d**. For the synthesis of the *N*-terminal variations set, a saponification of the methyl ester in **6** was carried out, yielding **7**, followed by a coupling reaction with benzylamine, leading to **8**. Further Boc-deprotection and formation of the acyl or urea derivatives (Table 1), followed by a final Cbz-deprotection, yielded analogues **10a**−**k** (Table 1). Analogue **14e** was obtained after Cbz-deprotection of **11** (Scheme 1). Compound **18** was synthesized starting from the reductive amination of **4** with D-Lys(2-ClCbz)$NHCH_2Ph$ (Scheme 2). Subsequent cyclization, Boc-deprotection, and coupling to phenylacetic acid yielded **17**, which was eventually deprotected to **18**. Mimetic **21** was obtained according to Scheme 3. All final products were purified with preparative HPLC resulting in purities of 98% and higher.

**Determination of Somatostatin Receptor Affinity Profiles.** All compounds were tested for their ability to bind to cell membrane pellet sections of cells expressing the five human

**Scheme 2**[a]

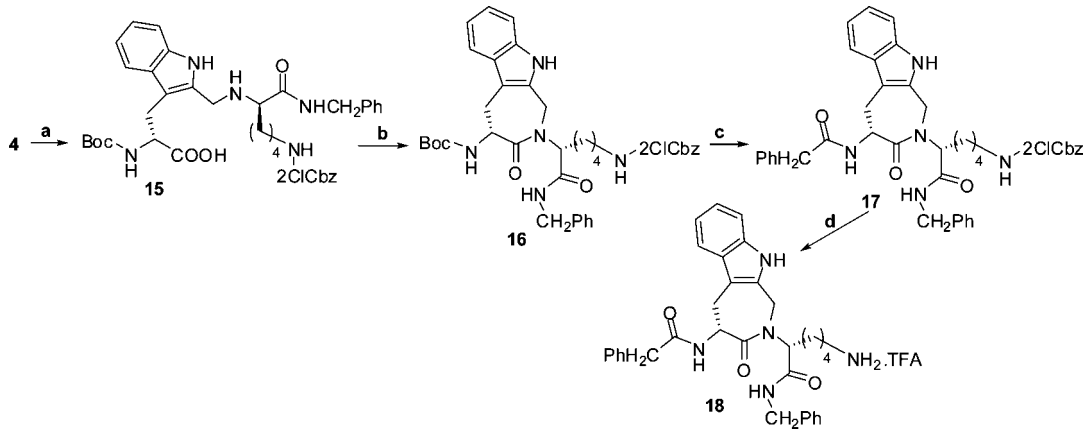

[a] Reagents and conditions: (a) D-Lys(2-ClCbz)NHCH$_2$Ph·TFA **22**, $CH_2Cl_2$, NMM, pH 6, $MgSO_4$, $NaBH_3CN$, 2 h; (b) EDC, pyridine, $CH_3CN$:$H_2O$ 1:1, high dilution, overnight; (c) (1) 0.5% $H_2O$ in TFA:$CH_3CN$ 2:1, 1 h; (2) $PhCH_2COOH$, $CH_2Cl_2$, $NEt_3$, TBTU, pH 8, 1 h; (d) EtOH, HCl, 10% Pd/C, $H_2$, 50 psi.

**Table 1.** Structure of *N*- and *C*-Terminal Substituents in **10** and **14**

| | $R_NC(O)$ | | $R_NC(O)$ | | $R_NC(O)$ | | $NH_2R_C$ |
|---|---|---|---|---|---|---|---|
| **10a** |  | **10e** | 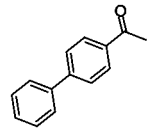 | **10i** | 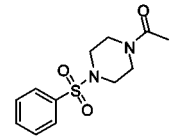 | **14a** | 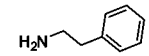 |
| **10b** | 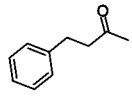 | **10f** | 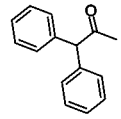 | **10j** | 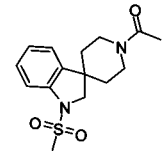 | **14b** | 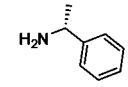 |
| **10c** |  | **10g** | 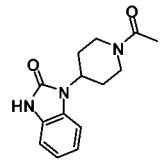 | **10k** | 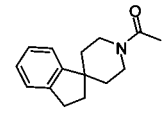 | **14c** | 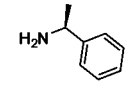 |
| **10d** | 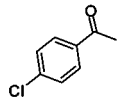 | **10h** | 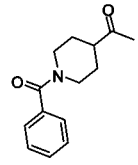 | | | **14d** | 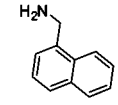 |

**Scheme 3**[a]

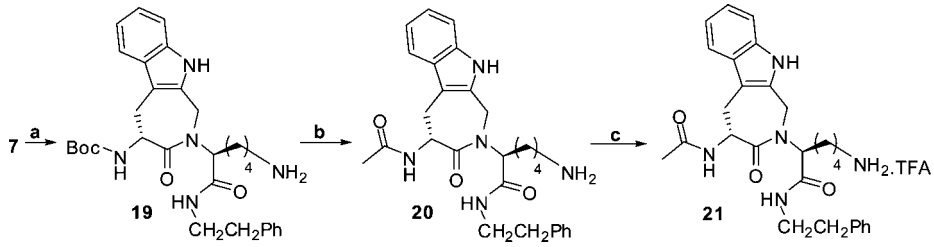

[a] Reagents and conditions: (a) $CH_2Cl_2$, $NEt_3$, TBTU, $PhCH_2CH_2NH_2$, pH 8, 1 h; (b) (1) 0.5% $H_2O$ in TFA:$CH_3CN$ 2:1, 1 h; (2) acetic anhydride, acetonitrile:water 1:1, $NEt_3$, pH 6, 2 h; (c) EtOH, HCl, 10% Pd/C, $H_2$, 50 psi.

sst receptor subtypes in complete displacement experiments using the universal somatostatin radioligand [$^{125}$I]-[Leu$^8$,D-Trp$^{22}$,Tyr$^{25}$]-somatostatin-28. The resulting binding affinities are shown in Table 2.

**Table 2.** Binding Affinities of the SRIF Peptide Mimetics

| | $IC_{50}$[a] (nM) | | | | |
|---|---|---|---|---|---|
| no. | $sst_1$ | $sst_2$ | $sst_3$ | $sst_4$ | $sst_5$ |
| **SS-28** | 1.9 ± 0.2 (12) | 2.0 ± 0.1 (12) | 1.7 ± 0.3 (12) | 2.0 ± 0.1 (12) | 2.6 ± 0.2 (12) |
| **2** | 233 ± 74 (3) | 83 ± 2 (3) | 251 ± 16 (3) | 3.3 ± 0.2 (3) | 1.2 ± 0.1 (3) |
| **10a** | 253 ± 73 (3) | 292 ± 91 (3)< | >1000 (3) | 7.0 ± 2.0 (3) | 5.0 ± 0.3 |
| **10b** | 54 ± 12 | 10 ± 1 | 153 ± 18 | 8.1 ± 0.8 | 3.4 ± 0.6 |
| **10c** | 27 ± 4 (3) | 103 ± 42 (3) | 182 ± 44 (3) | 1.3 ± 0.3 (3) | 1.8 ± 0.1 |
| **10d** | 38 ± 3 | 22 ± 2 | 162 ± 50 | 2.3 ± 0.1 | 3.7 ± 0.1 |
| **10e** | >1000 | 12 ± 2 | 54 ± 15 | 161 ± 75 | 16 ± 0.3 (2) |
| **10f** | 247 ± 42 | 242 ± 103 < | >500 | 14 ± 2 | 8.8 ± 1.3 |
| **10g** | 76 ± 3 (3) | 0.73 ± 0.23 (3) | 3.9 ± 1.0 | 4.4 ± 1.0 (3) | 0.86 ± 0.30 (3) |
| **10h** | 89 ± 7 (3) | 2.1 ± 0.2 (3) | 119 ± 16 (3) | 6.9 ± 1.7 (3) | 1.4 ± 0.3 (3) |
| **10i** | 372 ± 62 (3) | 4.2 ± 0.2 (3) | 260 ± 48 (3) | 59 ± 23 (3) | 3.5 ± 0.9 (3) |
| **10j** | 837 ± 47 (3) | 327 ± 88 (3) | 316 ± 75 (3) | 2.1 ± 0.5 | 8.0 ± 1.0 (3) |
| **10k** | 379 ± 90 (3) | 2.1 ± 0.7 (3) | 9.1 ± 3.0 | 35 ± 6 (3) | 2.9 ± 0.3 (3) |
| **14a** | 75 ± 15 (4) | 183 ± 52 (4) | 50 ± 5 (4) | 2.4 ± 0.5 (4) | 0.60 ± 0.22 (4) |
| **14b** | 630 ± 38 | 770 ± 177 | 403 ± 135 | 14 ± 1 | 50 ± 12 |
| **14c** | 183 ± 16 (3) | 452 ± 105 (3) | 300 ± 22 (3) | 1.0 ± 0.2 (3) | 3.2 ± 0.5 (3) |
| **14d** | 387 ± 94 (3) | 215 ± 56 (3) | 105 ± 13 (3) | 17 ± 2 (3) | 3.5 ± 1.1 (3) |
| **14e** | 962 ± 56 | 290 ± 45 | 400 ± 97 | 2.4 ± 0.9 | 13 ± 1 |
| **18** | >1000 < | >1000 | 910 ± 162 | 56 ± 7 | 25 ± 1 |
| **21** | 105 ± 15 (3) | >1000 (3) | 515 ± 87 (3) | 7.0 ± 1.4 (3) | 0.56 ± 0.20 (3) |

[a] The $IC_{50}$ values were derived from competitive radioligand displacement assays using the nonselective [$^{125}$]-[Leu$^8$, D-Trp$^{22}$, Tyr$^{25}$]-somatostatin-28 as radioligand. Mean values ± SEM; number in parenthesis represents number of experiments; all other values are $n + 2$.

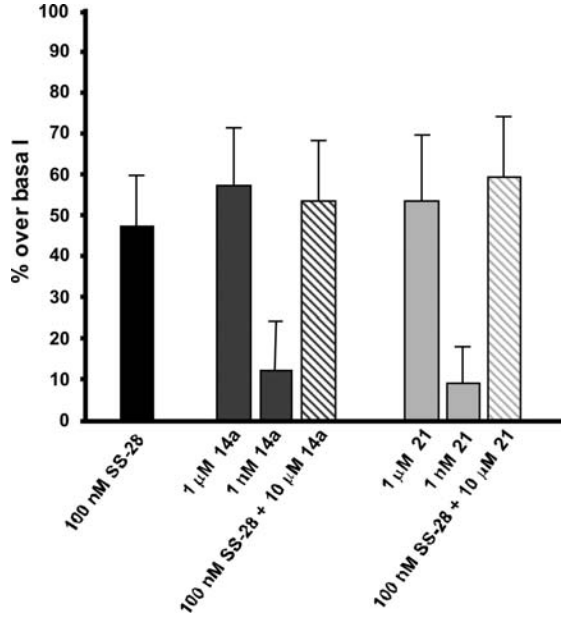


**Figure 2.** Effect on [$^{35}$S]GTP$\gamma$S Binding. The stimulation of [$^{35}$S]GTP$\gamma$S binding to sections of membrane pellets of CCL-$sst_5$ cells was performed as described in the Experimental Section. Sections of membrane pellets of CCL-$sst_5$ cells were treated either with 100 nM SS-28, 1 nM or 1 $\mu$M **14a**, 1 nM or 1 mM **21**, or 100 nM SS-28 in the presence of 10 mM **14a** or **21**. The bar-graphs represent the stimulated specific [$^{35}$S]GTP$\gamma$S binding over basal level and were obtained in three independent experiments in duplicates. The 1 nM conditions were performed twice in duplicates.

To further characterize the analogues with the highest $sst_5$ binding affinity, we functionally evaluated **14a** and **21** for agonism and antagonism in a [$^{35}$S]GTP$\gamma$S binding assay, using CCL-$sst_5$ cells, a cell line previously used by Hoyer and colleagues in a similar assay.[22] The specific binding of [$^{35}$S]GTP$\gamma$S to membrane pellet sections of CCL-$sst_5$ cells upon stimulation with **14a** or **21** alone or in the presence of SS-28 was determined by functional quantitative autoradiography. The data presented in Figure 2 show that **14a** and **21** stimulate [$^{35}$S]GTP$\gamma$S binding in a dose dependent manner but are not able to antagonize the 100 nM effect of SS-28. Thus **14a** and **21** are full agonists for the $sst_5$.

**Table 3.** Lowest Energy Conformers of **10g**

| conformation | $\Delta E$ pot (kcal/mol) | $\chi^1$ (D-Aia) (deg) | $\chi^2$ (D-Aia) (deg) | $\chi^1$ (Lys) (deg) |
|---|---|---|---|---|
| conf1 | 0.00 | −58 | −15 | −59 |
| conf2 | 0.71 | −55 | −19 | −60 |
| conf3 | 0.95 | −58 | −17 | −57 |
| conf4 | 1.03 | −55 | −21 | −57 |
| conf5 | 1.05 | 176 | 6 | −60 |

**Molecular Modeling.** The preferred conformations of the nonselective analogue **10g** and the $sst_5$-selective analogue **21** were studied by molecular modeling using Macromodel 5.0. The $\chi^2$, $\chi^3$, $\chi^4$, and $\chi^5$ of Lys were all fixed in the *trans* conformation. After the conformational search using the low mode (LMOD) method[23] with the GB/SA solvation model of Still et al.[24] in water and subsequent minimization, the resulting structures were clustered into families using an rmsd value of 0.2 Å. The lead structures of each family were considered and those greater than 5 kcal/mol above the global minimum were discarded. For both analogues, two values for the $\chi^1$ of D-Aia were found: *trans* and *gauche* (−) (g(−) for D-amino acids corresponds to g(+) for L-amino acids).

A total of 8378 conformations were found for **10g** (Table 3), of which 503 lead structures remained after clustering. Only structures with a potential energy of up to 5 kcal/mol above the global minimum were considered (63 conformations). Of those, 78% have $\chi^1$ (D-Aia) = *gauche* (−) and 22% have $\chi^1$ (D-Aia) = *trans*. For the Lys side chain, 49% has $\chi^1$ (Lys) = *gauche* (−) while in 35% a *trans* conformation is observed. Only 16% have the $\chi^1$ (Lys) = *gauche* (+). As is shown in Table 1, the lowest energy conformer of **10g** has $\chi^1$ (D-Aia) = *gauche* (−) and $\chi^1$ (Lys) = *gauche* (−), the first structure having a *trans* $\chi^1$ (D-Aia) being 1.05 kcal/mol above the global minimum.

A total of 2200 conformations were found for **21**, of which 423 lead structures remained after clustering. Conformations greater than 5 kcal/mol above the global minimum were discarded. The major part (84%) of the remaining structures (55) has the D-Aia side chain in *trans*, while the Lys $\chi^1$ is mainly *gauche* (−) (69%) or *trans* (27%). As can be seen from Table

**Table 4.** Lowest Energy Conformers of **21**

| conformation | $\Delta E$ pot (kcal/mol) | $\chi^1$ (D-Aia) (deg) | $\chi^2$ (d-Aia) (deg) | $\chi^1$ (Lys) (deg) |
|---|---|---|---|---|
| conf1 | 0.00 | 175 | 6 | −59 |
| conf2 | 0.29 | 176 | 5 | −60 |
| conf3 | 0.94 | 175 | 6 | −62 |
| conf4 | 1.17 | 175 | 6 | −60 |
| conf5 | 1.58 | 176 | 5 | −60 |

4, the lowest energy conformer of **21** has $\chi^1$ (D-Aia) = 175° and $\chi^1$ (Lys) = −59°. The first conformer with a *gauche* (−) conformation for the D-Aia side chain is 3.0 kcal/mol above the global minimum.

## Discussion

Starting from the structure of the previously reported highly potent SRIF mimetic **2**, new analogues containing the indolo[2,3-*c*]azepin-3-one ring system as a constraint for Trp were designed and synthesized. As can be seen from Table 2, *N*- and *C*-terminal variation of the substituents on the D-Aia-Lys scaffold results in analogues having a low nanomolar potency but a range of sst receptor subtype selectivities.

The importance of the aromatic moiety at the *N*-terminus in **2** was examined by removing it (analogue **10a**). As shown in Table 2, compared to **2**, the affinity of **10a** for $sst_1$ is retained while it has decreased for all the other receptors. Affinities for $sst_4$ and $sst_5$ are still in the low nanomolar range, showing that the aromatic residue at the *N*-terminus is not necessary for binding to $sst_4$ and $sst_5$. The length of the carbon chain was then investigated by extending it (**10b**) and shortening it (**10c**). In both cases, high affinity for $sst_4$ and $sst_5$ is retained while binding to $sst_{1-3}$ is increased compared to **2**. Apparently, the $sst_1$ receptor best accommodates the shorter benzoyl substituent in **12c** because it shows the highest increase in affinity (233 nM in **2** to 27 nM in **10c**). However, also the extension of the chain in **10b** results in a strong increase in $sst_1$ affinity (54 nM), which is in this case accompanied by an increase in $sst_2$ affinity (83 nM in **2** to 10 nM in **10b**). The introduction of a 4-chloro substituent in the benzoyl group, to give analogue **10d**, which was reported to increase mainly $sst_3$ affinity in a series of tryptophan-based mimetics,[25] significantly changed the affinity for $sst_2$ when compared to **10c**. In contrast, the introduction of a 4-phenyl substituent, leading to the biphenyl-4-carboxamide **10e**, has a more pronounced influence: the affinity for the $sst_{1,4,5}$ is substantially reduced, while that for $sst_{2,3}$ is markedly increased. This is consistent with the previously reported $sst_2$ selectivity of a biphenyl-4-carboxamide-substituted mimetic.[17]

A shortened version of **3**, analogue **10f**, was prepared. Compared to **3**, binding affinities toward $sst_{1,2,3}$ decreased. Mainly affinity for $sst_4$ increased while that for $sst_5$ was retained, resulting in a loss of $sst_5$ versus $sst_4$ selectivity. Compared to **2**, this analogue was less potent for all receptors.

As discussed above, none of the analogues resulting from variations of the phenylacetyl substituent in **2** showed an improved selectivity profile. The removal of the phenyl substituent to give acetyl-substituted analogue **10a** maintains the low nanomolar affinity for $sst_4$ and $sst_5$, but the benzoyl substituent in **10c** induces the highest potency at these receptors, but also at $sst_1$.

A set of *N*-terminal acyl and urea substituents, leading to analogues **10g**, **10h, 10i**, **10j**, and **10k**, was selected from potent $sst_2$-selective antagonists[17] and agonists[18−20,26,27] developed previously. These 4-substituted piperidine or piperazine substituents carry an aromatic ring that is intended to target the Phe[7] binding site. Accordingly, as is shown in Table 2, affinities for $sst_2$ of all these analogues, except **10j**, have increased tremendously compared to **2**, with subnanomolar $sst_2$ affinity for **10g**. This indicates that the set of *N*-terminal substituents that conferred high $sst_2$ affinity in the D-Trp-Lys scaffold is having a similar effect in the D-Aia-Lys scaffold and confirms that an aromatic residue corresponding to Phe[7] is important for $sst_2$ affinity. In general, a high potency at the $sst_5$ is maintained in all analogues. None of the analogues displayed high affinity for $sst_1$, but some showed low nanomolar affinity for $sst_3$ (**10g** and **10k**) or for $sst_4$ (**10b**, **10g**, **10h**, **10j**). Again, although some analogues in this *N*-terminal variations set showed high affinity for a particular receptor subtype, affinity for another subtype was always sufficiently high to prevent selectivity. As can be seen in Table 2, **10g** shows high potency for all receptors except $sst_1$. Only analogues **10i** and **10k** show a selectivity for $sst_5$ over $sst_4$ that is significantly higher than in **2**, but in each of those cases, selectivity of $sst_5$ over $sst_2$ or $sst_3$ is lost.

Some *C*-terminal variations were also examined (**14a**−**e**). In analogue **14a**, the alkyl chain of the benzyl amide is elongated with one carbon. Compared to **2**, this results in a decrease of $sst_2$ affinity while binding to all the other receptors is enhanced. The affinity for $sst_5$ is in the subnanomolar range, which is the highest of all analogues in this set. To explore the orientation of the aromatic moiety at the *C*-terminus, analogues **14b** and **14c** were designed. Whereas in **14b** a general loss of affinity for all receptors is observed, analogue **14c** becomes highly potent at $sst_4$, with however retention of substantial potency at $sst_5$.

The design of **14d** was based on a naphthyl containing $sst_5$-selective mimetic synthesized by Souers et al.[28] Compound **14d** shows a 2-fold decreased affinity for $sst_5$, but an improved $sst_5$ versus $sst_4$ selectivity compared to **2**. Surprisingly, the cyclic thioether $\beta$-turn mimetic described by Souers et al. had a preferred D-configuration for the Lys residue.[28] In our case, the D-Lys epimer of **2**, analogue **18**, showed a general large decrease of affinity, especially for $sst_1$ and $sst_2$.

Because several of the reported somatostatin mimetics contain a Lys methyl ester,[26,27,29] methyl ester **14e** was investigated. This resulted in a decrease of all binding affinities except toward $sst_4$, which results in an analogue that is quite selective except versus $sst_5$. The high binding affinities of phenylethylamide **14a** for $sst_{4,5}$ and the lower affinities for $sst_{1-3}$ of the *N*-acetylated **10a** led to the design of the *N*-acetyl-D-Aia-Lys-phenylethylamide analogue **21**. This mimetic indeed shows an excellent potency for $sst_5$ in the subnanomolar range, combined with a 10-fold selectivity of $sst_5$ over $sst_4$ and higher selectivities over the other receptors. **14a** and **21** have also been tested functionally in a [$^{35}$S]GTP$\gamma$S binding assay where they both behaved as full agonists. Analogue **21** confirms that the presence of an aromatic moiety at the *N*-terminus is not necessary for binding to $sst_4$ and $sst_5$. An iminosugar based $sst_4$-selective mimetic with affinity in the micromolar range was very recently reported by Chagnault et al.[30] Adding a benzyl substituent resulted in a substantial increase in $sst_5$ affinity, indicating that this aromatic residue makes an important binding interaction with $sst_5$ but not with $sst_4$. In our case, removing the aromatic moiety at the *N*-terminus does not have any influence on $sst_4$ or $sst_5$ binding affinities. This shows that hypotheses concerning SAR studies may be mimetic dependent, as was also observed above for the Lys configuration in the Souers mimetics.[27]

Only a few potent and $sst_5$-selective SRIF peptidic analogues have been reported: two cyclic peptides, PTR 3046, published by Gilon et al.[31] ($IC_{50}$ $sst_5$ = 67 nM), and a dicarba-containing analogue **23** recently reported by d'Addona et al.[32] ($IC_{50}$ $sst_5$ =

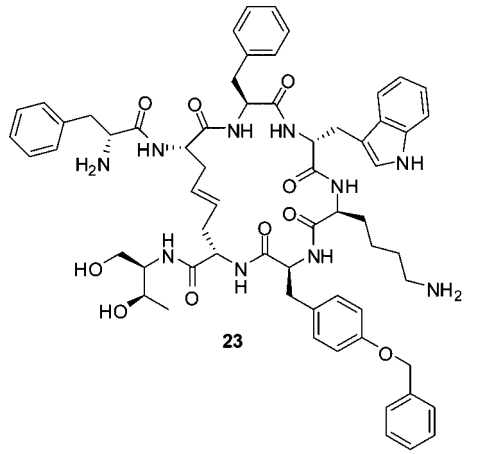

**23**

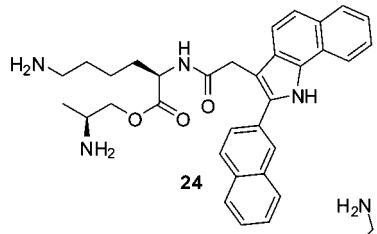

**24**

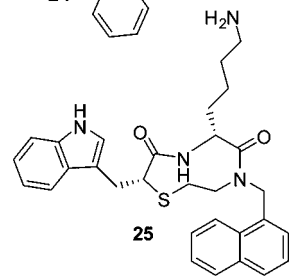

**25**

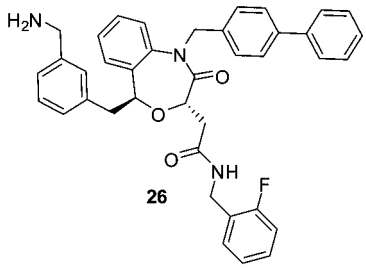

**26**

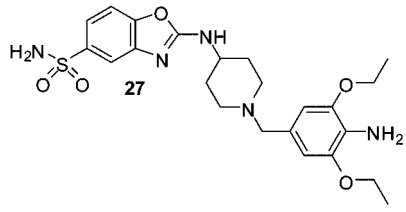

**27**

**Figure 3.** Previously reported $sst_5$-selective agonists and antagonist.

12 nM). These peptides show an excellent $sst_5$ selectivity (at least 24-fold), but their affinity toward $sst_5$ is at least 18 times less than in analogue **21**.

An $sst_5$-selective nonpeptidic mimetic **24** (Figure 3) was reported previously by Merck.[26] This analogue shows a subnanomolar affinity for $sst_5$ ($IC_{50} = 0.4$ nM) and the selectivity of $sst_5$ over $sst_1$ is 8-fold. The naphthyl containing thioether **25** (Figure 3), which was already mentioned,[28] has an affinity of 87 nM for $sst_5$ combined with a high selectivity of $sst_5$ over the other receptors. A benzoxazepine somatostatin mimetic **26** (Figure 3) was reported to have excellent $sst_5$ affinity ($IC_{50} =$ 0.3 nM) and a selectivity of 200 and more over the other receptor subtypes.[15,33] These three mimetics have all been shown to act

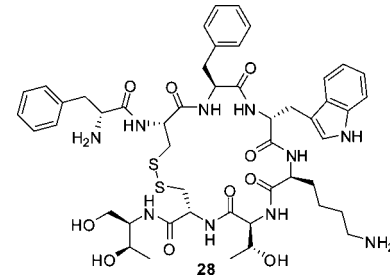

**28**

**Figure 4.** Octreotide **28**.

as agonists. Recently, the first class of $sst_5$-selective antagonists was designed at Hoffmann-La Roche by a chemogenomics approach.[34,35] The most potent analogue **27** ($K_i = 13$ nM) is shown in Figure 3. These comparisons confirm that **21** is one of the most potent $sst_5$-selective nonpeptidic mimetics reported to date exhibiting agonistic properties. Its selectivity profile is different from that of the previously reported $sst_5$-selective ligands.

**Conformational Analysis.** Many previously reported subtype selective cyclic peptide analogues contain a type II′ $\beta$-turn around the D-Trp[8]-Lys[9] residues and many somatostatin mimetics were designed on a $\beta$-turn mimetic template. A comprehensive conformational study on 4-amino-1,2,4,5-tetrahydro-2-benzazepin-3-ones showed that these structures do not adopt turn conformations but rather prefer an extended conformation.[36] An NMR study of **2** and **3** indeed indicated that these compounds do not adopt $\beta$-turns,[16] nevertheless, the upfield position of the Lys $C^{\gamma}H_2$, which is ascribed to a close proximity of the Trp and Lys side chains in the peptidic analogues and which correlates with high receptor affinity,[37] was observed. This upfield chemical shift of the Lys $\gamma$ protons is also observed in the newly synthesized compounds **10a**−**k**, **14a**−**e**, and **21** while it is absent in D-Lys containing **18**. This is reflected in the binding profiles, **18** is the analogue with the lowest binding affinities for all the receptors, with complete loss of binding to $sst_1$ and $sst_2$.

To better understand the high binding affinities of our analogues, despite the absence of a $\beta$-turn, compounds **10g** (nonselective analogue) and **21** ($sst_5$-selective) were subjected to a conformational analysis. The results were compared to data obtained for $sst_{2,3,5}$-selective octreotide **28**[38] (Figure 4) and the $sst_5$-selective dicarba-analogue **23** recently published by d'Addona et al.[32]

For analogue **10g**, the conformational search resulted in a lowest energy conformer with $\chi^1$ (D-Aia) $= -58°$ and $\chi^1$ (Lys) $= -59°$ (Table 3). Four more conformers were found within 1.1 kcal/mol above this global minimum, three of which have $\chi^1$ (D-Aia) in *gauche* (−) and one with $\chi^1$ (D-Aia) in *trans*. A *gauche* (−) value for the lysine side chain was found in all four. Because of coinciding signals of the azepinone and lysine alpha protons, NMR data in MeOD could not identify the $\chi^1$ value of D-Aia. The observed upfield shift of the lysine $\gamma$ protons however indicates a close proximity of these hydrogens with the indole ring, which is only possible when the D-Aia adopts a *trans* conformation. According to the molecular modeling, the first conformer with $\chi^1$ of D-Aia in *trans* has an energy of 1.05 kcal/mol above the global minimum, the majority (78%) having a *gauche* (−) conformation. This discrepancy may be due to a solvent effect but also indicates that **10g** can easily switch from a *trans* to a *gauche* (−) D-Aia conformation.

NMR data of **21** in MeOD clearly show that the solution conformation of this analogue has the $\chi^1$ (D-Aia) in *trans*. This

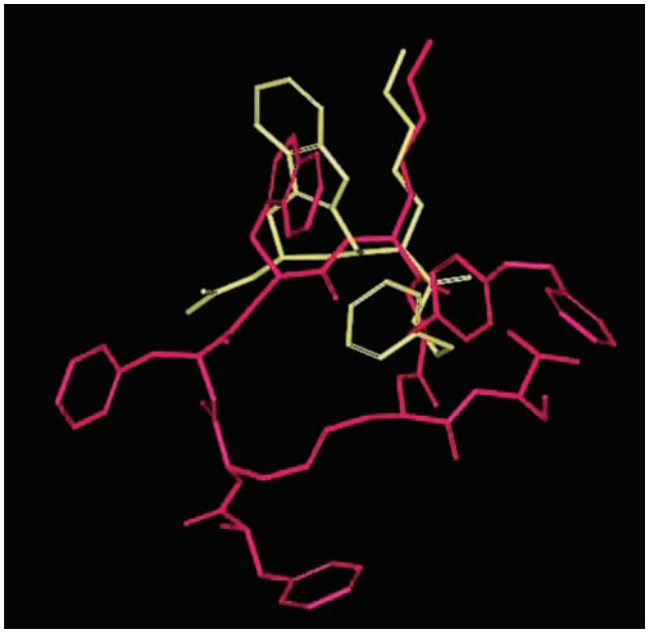

**Figure 5.** Superposition of **21** (yellow) with **23** (pink).

is in good agreement with the molecular modeling results (Table 4), where the five lowest energy conformers all have the $\chi^1$ of the D-Aia residue in *trans*. All these structures have the lysine side chain in *gauche* (−).

The most remarkable difference between **10g** and **21** is the different ability to adopt the *g*(−) conformation of the D-Aia residue. This increased flexibility of **10g** compared to **21** may allow it to adapt more easily to the different receptor subtypes.

For octreotide **28**, a conformational equilibrium is assumed based on NMR studies[38] as well as X-ray crystallography.[39] One conformer shows an antiparallel $\beta$-sheet structure while in the other two, the *C*-terminal residues form a $3_{10}$ helix-like fold. In both conformations, the D-Trp side chain adopts a *trans* conformation while the Lys $\chi^1$ is *gauche* (−) or *trans*. NMR studies on dicarba-analogues[32] such as **23** show a similar equilibrium and indicate that this equilibrium is shifted to the helical conformations in $sst_5$-selective analogues.

For octreotide **28**,[38] the proposed conformations of the Lys side chain are *gauche* (−) or *trans* as is the case for our analogues **10g** and **21**. The conformations found for **23** also have the lysine side chain in *gauche* (−).[32] The similarity between the $sst_5$-selective analogues **21** and **23** is reflected in the good backbone overlaps resulting from superimposing the lowest energy conformer of **21** (conf 1 in Table 4) with a representative NMR-derived conformation of **23** as is shown in Figure 5.

Superpositions of **10g** (Conf 5 in Table 3) with octreotide **28** also show a good overlap except for the *N*-terminal part (Figure 6).

Both analogues **10g** and **21** have similar values for the $\chi^1$ of the D-Trp and Lys residues. The cyclic nature of the Aia scaffold also results in a well defined $\chi^2$ value, which is different from the one proposed in **23** and octreotide but is consistent with the observed high field shift of the Lys $\gamma$ methylene protons in the NMR spectra. It can be mentioned that the D-Aia-Lys scaffold not only constrains the D-Trp side chain but also involves an alkylation of the Lys $N^{\alpha}$. $N^{\alpha}$-methylation of Lys[9] was shown not to cause dramatic effects on the receptor affinity and potency in octapeptide somatostatin agonists.[40] In contrast in an octapeptide somatostatin antagonist, it substantionally increased

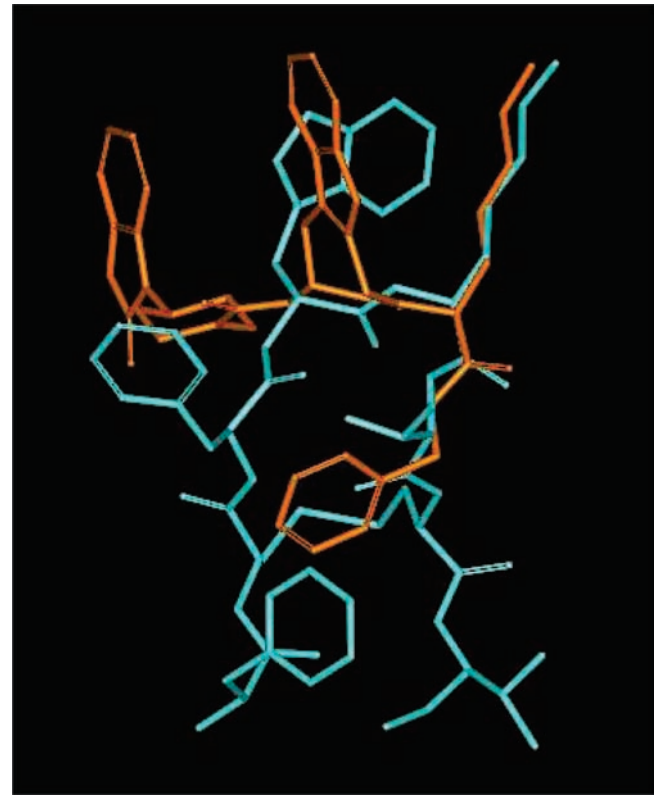

**Figure 6.** Superposition of **10g** (brown) with **28** (blue).

$sst_5$ affinity.[41] Therefore, the observed effect in the D-Aia-Lys analogues reported here, yielding a potent $sst_5$ agonist, may be mainly the result of the conformational constraint imposed by the D-Aia residue.

## Conclusion

On the basis of the structure of the potent $sst_{4,5}$-selective SRIF mimetic **2**, a series of new analogues was synthesized and their binding affinities for the five somatostatin receptors were determined. Depending on the *N*- or *C*-terminal substituents of the D-Aia-Lys dipeptide mimetic, potent analogues with a range of different subtype selectivities were obtained. Because some of the analogues show a low nanomolar affinity for each one of the receptor subtypes, except for $sst_1$, it can be concluded that the D-Aia-Lys scaffold represents a pharmacophore that is universally recognized by $sst_{2-5}$. The most interesting analogue is **21**, which shows a subnanomolar affinity for $sst_5$ and at least a 10-fold selectivity over the other receptors and behaves as a full agonist. $sst_5$-selective agonists may find important applications because the $sst_5$ receptor is believed to mediate the inhibition of growth hormone and adrenocorticotropin secretion.[42] It also inhibits insulin and amylase secretion in the pancreas. Some tumors like GH-expressing pituitary adenoma, kidney cancer, and thyroid cancer overexpress $sst_5$.[43,44] $sst_5$ has also been reported to play a role in learning and memory.[45]

A potent nonselective mimetic **10g** was identified. Analogues that bind equally well to all five subtypes are very interesting as drugs for long-term therapy in tumors that express several different somatostatin receptor subtypes. They can also be effective in nononcological indications characterized by disturbances of the physiological somatostatin system. When labeled with radioactive elements, they can identify tissues expressing all five subtypes.[46] Molecular modeling studies were carried out on **21** and **10g**, showing that these analogues have a different ability to adopt a *trans* or *gauche* (−) D-Aia side chain

conformation. The analogues reported here are the first examples of peptidomimetics in which the side chain conformation of the essential D-Trp residue has been constrained to allow only a limited range of $\chi^1$ and $\chi^2$ values. Many models for the bioactive conformation required for selective recognition by the somatostatin receptor subtypes have been proposed.[32,47−50] The results reported here should allow a better definition of the D-Trp orientation in these models and exclude the *gauche* (+) $\chi^1$ orientation.

## Experimental Section

**General.** Lys(ε-Cbz)OMe and Boc-D-Lys(ε-2-ClCbz)OH were purchased from Novabiochem (Läugelfinger, Switzerland). D-Lys(ε-2-ClCbz)$NHCH_2$Ph was synthesized using the standard procedures for amide formation and Boc-deprotection.[51] Boc-2′-formyl tryptophan **4** was prepared as described previously.[21] Synthesis and characterization of compound **8** were published previously.[16] Thin layer chromatography (TLC) was performed on plastic sheet precoated with silica gel $60F_{254}$ (Merck, Darmstadt, Germany) using specified solvent systems. Mass spectrometry (MS) was recorded on a VG Quattro II spectrometer using electrospray (ESP) ionization (positive or negative ion mode). Data collection was done with Masslynx software. Analytical RP-HPLC was performed using an Agilent 1100 Series system (Waldbronn, Germany) with a Supelco Discovery BIO Wide Pore (Bellefonte, PA, USA) RP C-18 column (25 cm × 4.6 mm, 5 μm) using UV detection at 215 nm. The mobile phase (system 1: water/acetonitrile, system 2: water/methanol) contained 0.1% TFA. The standard gradient consisted of a 20 min run from 3 to 97% acetonitrile (system 1) or methanol (system 2) at a flow rate of 1 mL/min. Preparative HPLC was performed on a Gilson apparatus and controlled with the software package Unipoint. The reverse phase C18-column (Discovery BIO Wide Pore 25 cm × 21.2 mm, 10 μm) was used under the same conditions as the analytical RP-HPLC, but with a flow rate of 20 mL $min^{-1}$. Nuclear magnetic resonance (NMR): $^1$H NMR and $^{13}$C NMR spectra were recorded at 250 and 63 MHz, respectively, on a Bruker Avance 250 spectrometer or at 500 and 125 MHz on a Bruker Avance II 500. Calibration was done with TMS (tetramethylsilane) or residual solvent signals as an internal standard. The solvent used is mentioned in all cases and the abbreviations used are: s (singlet), d (doublet), dd (double doublet), t (triplet), q (quadruplet), br s (broad singlet), m (multiplet), Lys (lysine protons), azep (azepinone protons), arom (aromatic protons). Optical rotations were measured on a Perkin-Elmer 241 polarimeter. Infrared spectral data were obtained using an Avatar 370 FT-IR.

**General Procedure for the Reductive Amination.** Boc-2′-formyl Trp **4** (1.0 g, 3.0 mmol) was suspended in dichloromethane (45 mL) and Lys(Cbz)OMe·HCl (1.05 equiv, 3.2 mmol, 1.04 g) or (D)Lys(2-ClCbz)NHBn·TFA (1.05 equiv, 3.2 mmol, 1.75 g) were added. The pH was adjusted to 6 by the addition of *N*-methyl morpholine. $MgSO_4$ (20 wt %, 0.20 g) and $NaBH_3CN$ (2.5 equiv, 7.5 mmol, 0.47 g) were added and the reaction was stirred at room temperature for 1.5 to 3 h.

The reaction mixture was evaporated and used without further purification in the cyclization reaction.

**General Procedure for the Cyclization. Synthesis of 6 and 16.** Crude amine **5** or **15** (9.0 mmol) was dissolved acetonitrile: water 1:1 (600 mL) and the solution was cooled to 0 °C. Pyridine (2.5 equiv, 22.5 mmol, 1.8 mL) and EDC·HCl (1.5 equiv, 13.5 mmol, 2.58 g) were added and the mixture was stirred at 0 °C for 1 h. Stirring was continued at room temperature overnight (**5**) or during 4 days (**15**, 3 more equiv of pyridine and EDC·HCl were added).

Acetonitrile was evaporated and 150 mL of EtOAc were added. The layers were separated and the organic phase was extracted with HCl (1M, 3 × 100 mL), $NaHCO_3$ (saturated, 3 × 100 mL) and brine (3 × 100 mL). The organic layer was dried over $MgSO_4$, and the crude mixture was purified by column chromatography (silica, EtOAc:$CH_2Cl_2$ gradient). Yield (**6**) = 37%. Yield (**16**) = 40%.

**General Procedure for the Boc-Deprotection.** Boc-protected amine (1.8 mmol) was dissolved in a TFA:water mixture (95:5, 13 mL) and acetonitrile was added (6 mL). The reaction was stirred for 1 h and the mixture was evaporated. Crude TFA-salts were used in the next reactions.

**General Procedure for the Saponification.** Methyl ester (4.05 mmol) was dissolved in MeOH (96 mL) and aqueous LiOH (1M, 4 equiv, 16.2 mmol, 16.2 mL) was added. The reaction was followed with TLC (silica, EtOAc) and after 1.5 h it was complete.

MeOH was evaporated and water (100 mL) and EtOAc (50 mL) were added. After extraction, the aqueous layer was acidified to pH 4 and extracted with EtOAc (3 × 50 mL). The organic layers were combined and washed with brine (3 × 100 mL). The organic phase was dried over $MgSO_4$, and after filtration, the mixture was evaporated.

**General Procedure for the Formation of Amide Bonds.** Acid (54 mmol) was dissolved in dry $CH_2Cl_2$ (250 mL). $NEt_3$ (3 equiv, 162 mmol, 22.5 mL) and TBTU (1.1 equiv, 59.4 mmol, 19.07 g) were added and the mixture was stirred at room temperature for 10 min. Amine TFA-salt (1.1 equiv, 59.4 mmol) was added and the pH was kept at 8 by the addition of $NEt_3$. The reaction was stirred for 1 h. The solution was extracted with HCl (1M, 3 × 80 mL), $NaHCO_3$ (saturated, 3 × 80 mL) and brine (3 × 80 mL). The organic layer was dried over $MgSO_4$, and after filtration, the residue was evaporated. No further purification was necessary.

**General Procedure for the Formation of Urea Bonds.** A suspension of amine TFA-salt (55.4 mmol), *N*,*N*′-disuccinimidyl carbonate (1.1 equiv, 60.9 mmol, 15.6 g) and *N*,*N*-diisopropylethylamine (2 equiv, 110.8 mmol, 18.3 mL) in $CH_2Cl_2$ (500 mL) was prepared. The solution was stirred at room temperature for 30 min, and a clear solution was formed. Piperidine or piperazine derivative (1 equiv, 55.4 mmol) was added and the pH was kept at 8 by the addition of DIEA. Stirring was continued overnight. The solution was extracted with HCl (1M, 3 × 15 mL), $NaHCO_3$ (saturated, 3 × 15 mL) and brine (3 × 15 mL). The organic layer was dried over $MgSO_4$, and after filtration, the solution was evaporated. No further purification was necessary.

**General Procedure for the Acetylation.** Amine TFA-salt (0.89 mmol) was dissolved in acetonitrile:water 1:1(10 mL) and the pH was adjusted to 6 by the addition of $NEt_3$. Acetic acid anhydride (5 equiv, 4.46 mmol, 0.42 mL) was added in three portions while the pH was kept at 6. The reaction was stirred for 2 h at room temperature. The solution was evaporated and after the addition of EtOAc (25 mL), it was extracted with HCl (1M, 3 × 15 mL), $NaHCO_3$ (saturated, 3 × 15 mL), and brine (3 × 15 mL). The organic layer was dried over $MgSO_4$, and after filtration, the solution was evaporated. No further purification was necessary.

**General Procedure for the Deprotection of Cbz and 2-Cl Cbz.** Cbz-protected compound (0.64 mmol) was dissolved in EtOH (50 mL). HCl (1equiv, 0.64 mmol, 0.064 mL) and 10% Pd/C (20 wt %) were added and the mixture was hydrogenated overnight in a Parr-apparatus at 20−50 psi. The catalyst was filtered off and the crude product was purified by preparative HPLC.

**Procedure for the Cbz-deprotection of 9d.** Dry HBr in AcOH (36%, 1.5 g) was added to Cbz-protected compound **9d** (0.41 mmol, 0.292 g). A $CaCl_2$-tube was put on the flask and the mixture was allowed to stand at room temperature for 1 h. Dry ether was added to precipitate the amine hydrobromide. The supernatant liquid was decanted and the solid triturated with ether, filtered, and washed with ether.

**Determination of Somatostatin Receptor Binding Affinity Profiles.** Cell membrane pellets were prepared and receptor autoradiography was performed on 20 μm thick pellet sections (mounted on microscope slides), as described in detail previously.[22,52] For each of the tested compounds, complete displacement experiments were performed with the universal somatostatin radioligand [$^{125}$I]-[Leu$^8$,D-Trp$^{22}$,Tyr$^{25}$]-somatostatin-28 (2000 Ci/mmol; Anawa, Wangen, Switzerland) using 15000 cpm/100 μL and increasing concentrations of the unlabeled compounds ranging from 0.1 to 1,000 nmol/L. Somatostatin-28 was run in parallel as control using the same increasing concentrations. $IC_{50}$ values were calculated after

quantification of the data using a computer-assisted image processing system.[22,52] Tissue standards containing known amounts of isotopes, cross-calibrated to tissue-equivalent ligand concentrations, were used for quantification.[52]

**[$^{35}$S]GTP$\gamma$S Binding Assay.** Chinese hamster lung fibroblasts (CCL39) stably expressing the human $sst_5$ (CCL-$sst_5$) were kindly provided by D. Hoyer (Novartis Pharma, Basel, Switzerland) and were grown in DMEM with GlutaMAX-I/Ham's F-12 Nut. Mix. with GlutaMAX-I (1:1) supplemented with 10% (v/v) fetal bovine serum, 100 U/mL penicillin, 100 $\mu$g/mL streptomycin, and 400 $\mu$g/mL Geneticin (G418-sulfate), and cultured at 37 °C and 5% $CO_2$. All culture reagents were from Gibco BRL, Life Technologies (Grand Island, NY). Cell membrane pellets of CCL-$sst_5$ were prepared as previously described and stored at −80 °C.[53] [$^{35}$S]GTP$\gamma$S binding assay was performed on 20 $\mu$m thick cryostat (Microm HM 500, Walldorf, Germany) sections of the membrane pellets, mounted on microscope slides. The sections were first preincubated for 10 min at room temperature in assay buffer (100 mM Tris-HCl buffer (pH 8.2), 1% BSA, 40 mg/L bacitracin 10 mM $MgCl_2$) and then for 30 min in assay buffer containing 50 $\mu$M GDP. Subsequently the sections were incubated for 2 h at room temperature in assay buffer containing 50 $\mu$M GDP, 40 pM (100000 cpm/ml) [$^{35}$S]GTP$\gamma$S (1250 Ci/mmol; PerkinElmer, Waltham, MA), and the absence (basal level) or presence (stimulated) of the compounds to be tested at the concentrations indicated. At the end of the incubation, the sections were washed on ice with assay buffer. After a brief dip in assay buffer without BSA and bacitracin to remove excess salts, the sections were dried and exposed to Kodak BioMax MR films. The relative optical densities of the pellets were determined using the MCID Basic 7.0 program (Imaging Research Inc.). Values were expressed as percentage over basal level.

**Molecular Modeling.** The calculations were carried out using Macromodel 5.0[54] with Maestro 8.0 as a graphic interface. Analogues **10g** and **21** were built using the following constraints: $\chi^2$ (Lys) = $\chi^3$ (Lys) = $\chi^4$ (Lys) = $\chi^5$ (Lys) = 180°. The MM3* force field[55] was used for energy minimization in combination with the GB/SA solvation model of Still et al.,[24] using MacroModel's default parameters for an aqueous medium. Conformational searches were carried out using the pure low mode search.[23] Structures were generated and minimized by means of the Polak-Ribière conjugate gradient method as implemented in MacroModel, using a gradient convergence criterion of 0.1 kJ/mol Å. The resulting conformations were again minimized to an energy convergence of 0.01 kJ/mol Å. Duplicate structures and those greater than 50 kJ/mol above the global minimum were discarded. The remaining structures were clustered into families using Xcluster 1.7. A rmsd value of 0.2 Å was used.

**Acknowledgment.** D. Feytens is a research assistant of the Fund for Scientic Research Flanders (FWO-Vlaanderen). We thank Dr. M. Kofod-Hansen from Novo Nordisk for a gift of 1,2-dihydro-1-methanesulfonyl spiro[3*H*-indole-3,4-piperidine]. Supported by FWO-grant no. G.0008.08. We thank Prof. A. Carotenuto for providing us the coordinates of **23**.

**Supporting Information Available:** Characterizations of compounds **6**−**22**. HPLC-purity data of compounds **6**−**22**. HPLC-chromatogram traces of compounds **10a**−**k**, **14a**−**e**, **18**, and **21**. This material is available free of charge via the Internet at http://pubs.acs.org.

## References

(1) Brazeau, P.; Vale, W.; Burgus, R.; Ling, N.; Butcher, M.; Rivier, J.; Guillemin, R. Hypothalamic polypeptide that inhibits secretion of immunoreactive pituitary growth-hormone. *Science* **1973**, *179*, 77–79.

(2) Janecka, A.; Zubrzycka, M.; Janecki, T. Somatostatin analogs. *J. Pept. Res.* **2001**, *58*, 91–107.

(3) Reichlin, S. Somatostatin 0.1. *New Engl. J. Med.* **1983**, *309*, 1495–1501.

(4) Reichlin, S. Somatostatin 0.2. *New Engl. J. Med.* **1983**, *309*, 1556–1563.

(5) Gillies, G. Somatostatin: The neuroendocrine story. *Trends Pharmacol. Sci.* **1997**, *18*, 87–95.

(6) Hoyer, D.; Bell, G. I.; Epelbaum, J.; Fenuik, W.; Humphrey, P. P. A.; O'Carroll, A.-M.; Patel, Y. C.; Schonbrunn, A.; Taylor, J. E.; Reisine, T. Classification and nomenclature of somatostatin receptors. *Trends Pharmacol. Sci.* **1995**, *16*, 86–88.

(7) Melacini, G.; Zhu, Q.; Osapay, G.; Goodman, M. A refined model for the somatostatin pharmacophore: conformational analysis of lanthionine-sandostatin analogs. *J. Med. Chem.* **1997**, *40*, 2252–2258.

(8) Veber, D. F. Design and discovery in the development of peptide analogs. In *Peptides, Chemistry and Biology: Proceedings of the 12th American Peptide Symposium, Cambridge, Massachusetts, June 16*−*21, 1991* ; Smith, J. A., Rivier, J. E., Eds.; ESCOM: Leiden, The Netherlands, 1992; pp 3−14.

(9) Bauer, W.; Briner, U.; Doepfner, W.; Haller, R.; Huguenin, R.; Marbach, P.; Petcher, T. J.; Pless, J. Sms 201−995− A very potent and selective octapeptide analog of somatostatin with prolonged action. *Life Sci.* **1982**, *31*, 1133–1140.

(10) Veber, D. F.; Freidinger, R. M.; Perlow, D. S.; Paleveda, W. J.; Holly, F. W.; Strachan, R. G.; Nutt, R. F.; Arison, B. H.; Homnick, C.; Randall, W. C.; Glitzer, M. S.; Saperstein, R.; Hirschmann, R. A potent cyclic hexapeptide analog of somatostatin. *Nature* **1981**, *292*, 55–58.

(11) Dalm, V. A. S. H.; Hofland, L. J.; Lamberts, S. W. J. Future clinical prospects in somatostatin/cortistatin/somatostatin receptor field. *Mol. Cell. Endocrinol.* **2008**, *286*, 262–277.

(12) Wolkenberg, S. E.; Thut, C. J. Recent progress in the discovery of selective, nonpeptide ligands of somatostatin receptors. *Curr. Opin. Drug Discovery Dev.* **2008**, *11*, 446–457.

(13) Jones, R. M.; Boatman, P. D.; Semple, G.; Shin, Y. J.; Tamura, S. Y. Clinically validated peptides as templates for de novo peptidomimetic drug design at G-protein-coupled receptors. *Curr. Opin. Pharmacol.* **2003**, *3*, 530–543.

(14) Weckbecker, G.; Lewis, I.; Albert, R.; Schmid, H. A.; Hoyer, D.; Bruns, C. Opportunities in somatostatin research: Biological, chemical and therapeutic aspects. *Nat. Rev. Drug Discovery* **2003**, *2*, 999–1017.

(15) Yang, L. H. Nonpeptide somatostatin receptor ligands. *Annu. Rep. Med. Chem.* **1999**, *34*, 209–218.

(16) Feytens, D.; Cescato, R.; Reubi, J. C.; Tourwe, D. New sst(4/5)-selective somatostatin peptidomimetics based on a constrained tryptophan scaffold. *J. Med. Chem.* **2007**, *50*, 3397–3401.

(17) Hay, B. A.; Cole, B. M.; DiCapua, F.; Kirk, G. W.; Murray, M. C.; Nardone, R. A.; Pelletier, D. J.; Ricketts, A. P.; Robertson, A. S.; Siegel, T. W. Small molecule somatostatin receptor subtype-2 antagonists. *Bioorg. Med. Chem. Lett.* **2001**, *11*, 2731–2734.

(18) Yang, L. H.; Berk, S. C.; Rohrer, S. P.; Mosley, R. T.; Guo, L. Q.; Underwood, D. J.; Arison, B. H.; Birzin, E. T.; Hayes, E. C.; Mitra, S. W.; Parmar, R. M.; Cheng, K.; Wu, T. J.; Butler, B. S.; Foor, F.; Pasternak, A.; Pan, Y. P.; Silva, M.; Freidinger, R. M.; Smith, R. G.; Chapman, K.; Schaeffer, J. M.; Patchett, A. A. Synthesis and biological activities of potent peptidomimetics selective for somatostatin receptor subtype 2. *Proc. Natl. Acad. Sci. U.S.A.* **1998**, *95*, 10836–10841.

(19) Yang, L. H.; Pan, Y. P.; Guo, L. Q.; Morriello, G.; Pasternak, A.; Rohrer, S.; Schaeffer, J.; Patchett, A. A. The design and synthesis of nonpeptide somatostatin receptor agonists. In *Peptides for the new millennium: Proceedings of the 16th American Peptide Symposium, Minneapolis, Minnesota, June 26-July 1, 1999*; Tam, G. A., Barany, G., Eds.; Kluwer: Dordrecht, The Netherlands, 2000; pp250−252.

(20) Zhou, C. Y.; Guo, L. Q.; Morriello, G.; Pasternak, A.; Pan, Y. P.; Rohrer, S. P.; Birzin, E. T.; Huskey, S. E. W.; Jacks, T.; Schleim, K. D.; Cheng, K.; Schaeffer, J. M.; Patchett, A. A.; Yang, L. H. Nipecotic and isonipecotic amides as potent and selective somatostatin subtype-2 receptor agonists. *Bioorg. Med. Chem. Lett.* **2001**, *11*, 415–417.

(21) Pulka, K.; Feytens, D.; Van den Eynde, I.; De Wachter, R.; Kosson, P.; Misicka, A.; Lipkowski, A.; Chung, N. N.; Schiller, P. W.; Tourwe, D. Synthesis of 4-amino-3-oxo-tetrahydroazepino[3,4-*b*]indoles: new conformationally constrained Trp analogs. *Tetrahedron* **2007**, *63*, 1459–1466.

(22) Siehler, S.; Hoyer, D. Characterisation of human recombinant somatostatin receptors. 4. Modulation of phospholipase C activity. *Naunyn-Schmiedebergs Arch. Pharmacol.* **1999**, *360*, 522–532.

(23) Kolossvary, I.; Guida, W. C. Low mode search. An efficient, automated computational method for conformational analysis: Application to cyclic and acyclic alkanes and cyclic peptides. *J. Am. Chem. Soc.* **1996**, *118*, 5011–5019.

(24) Still, W. C.; Tempczyk, A.; Hawley, R. C.; Hendrickson, T. Semianalytical treatment of solvation for molecular mechanics and dynamics. *J. Am. Chem. Soc.* **1990**, *112*, 6127–6129.

(25) Moinet, C.; Contour-Galcera, M. O.; Poitout, L.; Morgan, B.; Gordon, T.; Roubert, P.; Thurieau, C. Novel nonpeptide ligands for the somatostatin sst(3) receptor. *Bioorg. Med. Chem. Lett.* **2001**, *11*, 991–995.

(26) Rohrer, S. P.; Birzin, E. T.; Mosley, R. T.; Berk, S. C.; Hutchins, S. M.; Shen, D. M.; Xiong, Y. S.; Hayes, E. C.; Parmar, R. M.; Foor, F.; Mitra, S. W.; Degrado, S. J.; Shu, M.; Klopp, J. M.; Cai, S. J.; Blake, A.; Chan, W. W. S.; Pasternak, A.; Yang, L. H.; Patchett, A. A.; Smith, R. G.; Chapman, K. T.; Schaeffer, J. M. Rapid identification of subtype-selective agonists of the somatostatin receptor through combinatorial chemistry. *Science* **1998**, *282*, 737–740.

(27) Souers, A. J.; Rosenquist, A.; Jarvie, E. M.; Ladlow, M.; Feniuk, W.; Ellman, J. A. Optimization of a somatostatin mimetic via constrained amino acid and backbone incorporation. *Bioorg. Med. Chem. Lett.* **2000**, *10*, 2731–2733.

(28) Souers, A. J.; Virgilio, A. A.; Rosenquist, A.; Fenuik, W.; Ellman, J. A. Identification of a potent heterocyclic ligand to somatostatin receptor subtype 5 by the synthesis and screening of beta-turn mimetic libraries. *J. Am. Chem. Soc.* **1999**, *121*, 1817–1825.

(29) Berk, S. C.; Rohrer, S. P.; Degrado, S. J.; Birzin, E. T.; Mosley, R. T.; Hutchins, S. M.; Pasternak, A.; Schaeffer, J. M.; Underwood, D. J.; Chapman, K. T. A combinatorial approach toward the discovery of nonpeptide, subtype-selective somatostatin receptor ligands. *J. Comb. Chem.* **1999**, *1*, 388–396.

(30) Chagnault, V.; Lalot, J.; Murphy, P. V. Synthesis of somatostatin mimetics based on 1-deoxynojirimycin. *ChemMedChem* **2008**, *3*, 1071–1076.

(31) Gilon, C.; Huenges, M.; Matha, B.; Gellerman, G.; Hornik, V.; Afargan, M.; Amitay, O.; Ziv, O.; Feller, E.; Gamliel, A.; Shohat, D.; Wanger, M.; Arad, O.; Kessler, H. A backbone-cylic, receptor 5-selective somatostatin analogue: Synthesis, bioactivity, and nuclear magnetic resonance conformational analysis. *J. Med. Chem.* **1998**, *41*, 919–929.

(32) D'Addona, D.; Carotenuto, A.; Novellino, E.; Piccand, V.; Reubi, J. C.; Di Cianni, A.; Gori, F.; Papini, A. M.; Ginanneschi, M. Novel sst(5)-selective somatostatin dicarba-analogues: synthesis and conformation−affinity relationships. *J. Med. Chem.* **2008**, *51*, 512–520.

(33) Mabuchi, H.; Suzuki, N.; Miki, T. WO 98/47882 A1, 1998.

(34) Guba, W.; Green, L. G.; Martin, R. E.; Roche, O.; Kratochwil, N.; Mauser, H.; Bissantz, C.; Christ, A.; Stahl, M. From astemizole to a novel hit series of small-molecule somatostatin 5 receptor antagonists via GPCR affinity profiling. *J. Med. Chem.* **2007**, *50*, 6295–6298.

(35) Martin, R. E.; Green, L. G.; Guba, W.; Kratochwil, N.; Christ, A. Discovery of the first nonpeptidic, small-molecule, highly selective somatostatin receptor subtype 5 antagonists: A chemogenomics approach. *J. Med. Chem.* **2007**, *50*, 6291–6294.

(36) Van Rompaey, K.; Ballet, S.; Tomboly, C.; De Wachter, R.; Vanommeslaeghe, K.; Biesemans, M.; Willem, R.; Tourwe, D. Synthesis and evaluation of the beta-turn properties of 4-amino-1,2,4,5-tetrahydro-2-benzazepin-3-ones and of their spirocyclic derivative. *Eur. J. Org. Chem.* **2006**, 2899–2911.

(37) Arison, B. H.; Hirschmann, R.; Veber, D. F. Inferences about the conformation of somatostatin at a biologic receptor based on nmr-Studies. *Bioorg. Chem.* **1978**, *7*, 447–451.

(38) Melacini, G.; Zhu, Q.; Goodman, M. Multiconformational NMR analysis of sandostatin (octreotide): equilibrium between beta-sheet and partially helical structures. *Biochemistry* **1997**, *36*, 1233–1241.

(39) Pohl, E.; Heine, A.; Sheldrick, G. M.; Dauter, Z.; Wilson, K. S.; Kallen, J.; Huber, W.; Pfaffli, P. J. Structure of octreotide, a somatostatin analog. *Acta Crystallogr., Sect. D: Biol. Crystallogr.* **1995**, *51*, 48–59.

(40) Rajeswaran, W. G.; Hocart, S. J.; Murphy, W. A.; Taylor, J. E.; Coy, D. H. *N*-Methyl scan of somatostatin octapeptide agonists produces interesting effects on receptor subtype specificity. *J. Med. Chem.* **2001**, *44*, 1416–1421.

(41) Rajeswaran, W. G.; Hocart, S. J.; Murphy, W. A.; Taylor, J. E.; Coy, D. H. Highly potent and subtype selective ligands derived by *N*-methyl scan of a somatostatin antagonist. *J. Med. Chem.* **2001**, *44*, 1305–1311.

(42) van der Hoek, J.; Waaijers, M.; van Koetsveld, P. M.; Sprij-Mooij, D.; Feelders, R. A.; Schmid, H. A.; Schoeffter, P.; Hoyer, D.; Cervia, D.; Taylor, J. E.; Culler, M. D.; Lamberts, S. W. J.; Hofland, L. J. Distinct functional properties of native somatostatin receptor subtype 5 compared with subtype 2 in the regulation of ACTH release by corticotroph tumor cells. *Am. J. Physiol. Endocrinol. Metab.* **2005**, *289*, E278–E287.

(43) Froidevaux, S.; Eberle, A. N. Somatostatin analogs and radiopeptides in cancer therapy. *Biopolymers* **2002**, *66*, 161–183.

(44) Reubi, J. C. Peptide receptors as molecular targets for cancer diagnosis and therapy. *Endocr. Rev.* **2003**, *24*, 389–427.

(45) Pittaluga, A.; Feligioni, M.; Longordo, F.; Arvigo, M.; Raiteri, M. Somatostatin-induced activation and up-regulation of *N*-methyl-D-aspartate receptor function: Mediation through calmodulin-dependent protein kinase II, phospholipase C, protein kinase C, and tyrosine kinase in hippocampal noradrenergic nerve endings. *J. Pharmacol. Exp. Ther.* **2005**, *313*, 242–249.

(46) Reubi, J. C.; Eisenwiener, K. P.; Rink, H.; Waser, B.; Macke, H. R. A new peptidic somatostatin agonist with high affinity to all five somatostatin receptors. *Eur. J. Pharmacol.* **2002**, *456*, 45–49.

(47) Grace, C. R. R.; Koerber, S. C.; Erchegyi, J.; Reubi, J. C.; Rivier, J.; Riek, R. Novel sst(4)-selective somatostatin (SRIF) agonists. 4. Three-dimensional consensus structure by NMR. *J. Med. Chem.* **2003**, *46*, 5606–5618.

(48) Grace, C. R. R.; Durrer, L.; Koerber, S. C.; Erchegyi, J.; Reubi, J. C.; Rivier, J. E.; Riek, R. Somatostatin receptor 1 selective analogues: 4. Three-dimensional consensus structure by NMR. *J. Med. Chem.* **2005**, *48*, 523–533.

(49) Grace, C. R. R.; Erchegyi, J.; Koerber, S. C.; Reubi, J. C.; Rivier, J.; Riek, R. Novel sst(2)-selective somatostatin agonists. Three-dimensional consensus structure by NMR. *J. Med. Chem.* **2006**, *49*, 4487–4496.

(50) Nikiforovich, G. V.; Marshall, G. R.; Achilefu, S. Molecular modeling suggests conformational scaffolds specifically targeting five subtypes of somatostatin receptors. *Chem. Biol. Drug Des.* **2007**, *69*, 163–169.

(51) Damour, D.; Herman, F.; Labaudiniere, R.; Pantel, G.; Vuilhorgne, M.; Mignani, S. Synthesis of novel proline and gamma-lactam derivatives as nonpeptide mimics of Somatostatin/Sandostatin (R). *Tetrahedron* **1999**, *55*, 10135–10154.

(52) Cescato, R.; Erchegyi, J.; Waser, B.; Piccand, V.; Maecke, H. R.; Rivier, J. E.; Reubi, J. C. Design and in vitro characterization of highly sst(2)-selective somatostatin antagonists suitable for radiotargeting. *J. Med. Chem.* **2008**, *51*, 4030–4037.

(53) Reubi, J. C.; Schar, J. C.; Waser, B.; Wenger, S.; Heppeler, A.; Schmitt, J. S.; Macke, H. R. Affinity profiles for human somatostatin receptor subtypes SST1-SST5 of somatostatin radiotracers selected for scintigraphic and radiotherapeutic use. *Eur. J. Nucl. Med.* **2000**, *27*, 273–282.

(54) Mohamadi, F.; Richards, N. G. J.; Guida, W. C.; Liskamp, R.; Lipton, M.; Caufield, C.; Chang, G.; Hendrickson, T.; Still, W. C. Macromodel−an integrated software system for modeling organic and bioorganic molecules using molecular mechanics. *J. Comput. Chem.* **1990**, *11*, 440–467.

(55) Allinger, N. L.; Yuh, Y. H.; Lii, J. H. Molecular mechanics−the MM3 force-field for hydrocarbons 0.1. *J. Am. Chem. Soc.* **1989**, *111*, 8551–8566.

JM801205X